

Crossing point of the magnetization versus temperature curves and the Meissner fraction in granular $\text{La}_{1.9}\text{Sr}_{0.1}\text{CuO}_4$ superconductors: Random orientation and inhomogeneity effects

J. Mosqueira and M. V. Ramallo

Laboratorio de Bajas Temperaturas y Superconductividad, Departamento de Física de la Materia Condensada, Universidad de Santiago de Compostela, E15706, Spain

A. Revcolevschi

Laboratoire de Chimie des Solides, Université Paris XI, F91405 Orsay Cedex, France

C. Torrón and Félix Vidal

Laboratorio de Bajas Temperaturas y Superconductividad, Departamento de Física de la Materia Condensada, Universidad de Santiago de Compostela, E15706, Spain

(Received 22 June 1998)

In this paper, we first calculate the extrinsic random orientation effects on the Meissner fraction in granular layered superconductors with highly anisotropic single crystal grains. Then we present detailed measurements of the crossing point of the excess magnetization versus temperature curves, $\Delta M(T)_H$, in the reversible mixed state and of the Meissner fraction in two granular $\text{La}_{1.9}\text{Sr}_{0.1}\text{CuO}_4$ samples, before and after grain alignment. The analyses of these experiments on the grounds of the calculations indicated above allow us to disentangle the different extrinsic effects on the excess magnetization at the crossing point, ΔM^* , and on the field-cooled susceptibility at the crossing point temperature, $\chi^{\text{FC}}(T^*)$: random orientation, demagnetization, and inhomogeneities. We show then that once these two measured observables are adequately and separately corrected from random orientation and demagnetizing effects, the remaining extrinsic effects on ΔM^* (associated with structural and, mainly, stoichiometric inhomogeneities) may be taken into account through $\chi^{\text{FC}}(T^*)$. This seems to apply at least in samples with relatively good magnetic response [let us say, with $|\chi_{ab}^{\text{FC}}(T^*)| \geq 0.2$]. The resulting intrinsic crossing point may be explained in terms of the theoretical approaches proposed by Bulaevskii and co-workers and by Tešanović and co-workers and based on thermal fluctuations of vortices. These last results extend to granular high-temperature superconductors (HTSC) our recent conclusions for highly anisotropic single crystalline HTSC. [S0163-1829(99)09405-9]

I. INTRODUCTION

One of the most striking manifestations of the thermal fluctuations of magnetic vortices in highly-anisotropic high-temperature superconductors (HTSC) is the appearance of the so-called ‘‘crossing point’’ of the excess magnetization versus temperature curves in the reversible mixed state:¹⁻⁷ a few degrees below the mean-field-like transition temperature T_{c0} , the excess magnetization versus temperature curves for different amplitudes of the magnetic field (H) applied perpendicularly to the superconducting CuO_2 (ab) layers, $\Delta M_{ab}(T)_H$, cross at a point of coordinates ΔM_{ab}^* and T^* . Here the in-plane excess magnetization (for H perpendicular to the ab planes) is defined as $\Delta M_{ab}(T, H) = M_{ab}(T, H) - M_{abB}(T, H)$, where the background magnetization, $M_{abB}(T, H)$, is the magnetization associated with the normal contributions. $M_{abB}(T, H)$ may be approximated by extrapolating through the transition the magnetization measured above T_{c0} , in a temperature region where the effects of thermal fluctuations become negligible.

Soon after its first experimental observation,^{1,2} it was proposed by Bulaevskii and co-workers⁸ (BLK approach) and by Tešanović and co-workers⁹ (TXBLS approach) that the crossing point of the excess magnetization versus temperature curves could be due to thermal fluctuations of the vortex positions and, respectively, of the vortex number. The rela-

tive importance of these two different contributions depends on the strength of the applied magnetic field relative to both $H_{c2}(T^*)$, the in-plane upper critical field at T^* , and H_0 , the so-called dimensional-crossover field in anisotropic layered superconductors.⁸⁻¹⁰ Both theoretical approaches predict that the crossing point coordinates are related by¹¹

$$\Delta M_{ab}^* = - \frac{k_B T^*}{\phi_0 s_e^V}, \quad (1)$$

where k_B is the Boltzmann constant and s_e^V is an effective periodicity length which takes into account the possible multilayering effects on the vortex fluctuations. s_e^V may be related to the effective number, N_e^V , of fluctuating layers in the crystallographic periodicity, s (which in HTSC is equal to the unit cell length in the c direction if the cell is primitive, or half of that if it is body centered), through, $s_e^V = s/N_e^V$. Moreover, it is expected that $1 \leq N_e^V \leq N$, and then that $s/N \leq s_e^V \leq s$, where N is the number of superconducting CuO_2 layers in s . Note already here that in the $\text{La}_{1.9}\text{Sr}_{0.1}\text{CuO}_4$ (LaSCO) samples studied here $N=1$ and, therefore, s_e^V is expected to be equal to s .

The importance of Eq. (1) is enhanced by the fact that it relates directly the effective periodicity length, s_e^V , a microscopic parameter which in multilayered HTSC may depend on the Josephson and on the magnetic couplings between

adjacent superconducting layers, to two directly measurable macroscopic observables, ΔM_{ab}^* and T^* . This theoretical result has led, therefore, to much experimental activity.³⁻⁷ However, all the $\Delta M^*/T^*$ data published until now in polycrystalline or in single crystalline HTSC strongly disagree, in both the amplitude and the s dependence, with Eq. (1). In particular, in most of the experiments the measured $\Delta M_{ab}^*/T^*$ leads to an effective periodicity length, s_e^V , larger than s , in contradiction with the theoretical predictions.³⁻⁷ The presence of strong stoichiometric inhomogeneities, which will appreciably reduce the superconducting fraction, has been discarded in most of the studied samples by independent measurements (x-ray and neutron diffraction, in particular).⁴⁻⁷ Therefore, until now most of the authors propose that these $\Delta M_{ab}^*/T^*$ data are intrinsic and that the BLK and the TXBLS approaches do not explain, even at a qualitative level, the crossing points observed in highly anisotropic HTSC.^{3-6,12,13} It has been proposed recently, however, that this important and long standing problem could be resolved by taking into account all the possible nonintrinsic effects on the magnetization.⁷ These nonintrinsic effects will be associated with structural and stoichiometric inhomogeneities, at different length scales and amplitudes, and not only with those due to the presence of strong stoichiometric inhomogeneities at long length scales (i.e., at length scales much larger than the superconducting coherence lengths, which are those easily observable with conventional x-ray and neutron diffraction techniques). This conclusion was strongly supported by simultaneous measurements of the crossing point in the high magnetic field limit [$H \lesssim H_{c2}(T^*)$; $H \gg H_0$] and of the field-cooled susceptibility (the so called Meissner fraction), χ_{ab}^{FC} , in different single crystals of various highly anisotropic HTSC families with different values of N and s : For each crystal, the differences between the measured ΔM_{ab}^* and the in-plane excess magnetization predicted by Eq. (1), with $s_e^V = s$, were found to be similar to the differences between the measured χ_{ab}^{FC} (corrected from demagnetizing effects) and the total flux expulsion ($\chi_{ab}^{FC} = -1$).¹⁴ This conclusion seems to apply at least in crystals with relatively good magnetic response [in particular, with $|\chi_{ab}^{FC}(T^*)| \geq 0.2$]. In other words, the results of Ref. 14 demonstrate experimentally that in high quality anisotropic HTSC crystals $\Delta M_{ab}^*/|\chi_{ab}^{FC}(T^*)|$ verifies, within the experimental uncertainties, Eq. (1), with $s_e^V = s$, independently of N . Complementarily, these results show that in spite of the fact that ΔM_{ab}^* and $\chi_{ab}^{FC}(T^*)$ are measured under very different magnetic field amplitudes [$H \lesssim H_{c2}(T^*)$ and, respectively, $H \lesssim H_{c1}(T^*)$, the lower critical magnetic field at T^*], the nonintrinsic effects on both observables, associated with stoichiometric and structural inhomogeneities at different length scales, are the same within the experimental uncertainties. $\Delta M_{ab}^*/|\chi_{ab}^{FC}(T^*)|$ is, therefore, the intrinsic excess magnetization coordinate of the crossing point.

It is worthwhile wondering now how the above results on the crossing point and on the Meissner fraction, obtained on very good single crystals and for a magnetic field applied perpendicularly to the ab planes are affected by the random orientations of the grains in polycrystalline and granular samples. In particular, is the Meissner fraction also the adequate correction to introduce in order to obtain the *intrinsic*

excess magnetization at the crossing point in granular, with randomly oriented single crystalline grains, highly anisotropic HTSC? In addition to their importance for the understanding of the vortex thermal fluctuation effects in polycrystalline and granular highly anisotropic HTSC, these questions also concern central aspects of the interplay between structural and stoichiometric inhomogeneities and random orientation effects on the magnetization in these granular materials. To answer these questions, in Sec. II we first calculate the intrinsic (associated with the intrinsic anisotropy of the HTSC) and extrinsic (associated with the extrinsic anisotropy of the magnetic flux trapping) random orientation effects on the magnetization of granular samples with anisotropic single crystalline grains randomly oriented with respect to an applied magnetic field. These results are then used to analyze detailed measurements of the crossing point and of the Meissner fraction of two granular $\text{La}_{1.9}\text{Sr}_{0.1}\text{CuO}_4$ (LaSCO) samples with randomly oriented grains and after magnetic orientation of the grains. In this way, the random orientation effects on both observables are separated from the effects due to stoichiometric and structural inhomogeneities. Let us also stress already here that the choice of LaSCO samples was mainly motivated by the fact that, as indicated before, this HTSC family has only one superconducting CuO_2 layer per periodicity length ($N=1$). Therefore, the possible complications associated with the multilayering effects are absent in this case, i.e., $s_e^V = s$ in Eq. (1). These measurements will be shown in Sec. III, whereas the corresponding analyses will be presented in Sec. IV. The conclusions are summarized in Sec. V.

II. THE AVERAGE MAGNETIZATION OF GRANULAR HTSC AT THE CROSSING POINT AND IN THE MEISSNER REGION

The magnetization of a granular sample with anisotropic single crystalline grains randomly oriented may be related to $M_L(\theta, \varphi)$, the longitudinal component (along the applied magnetic field) of the magnetization vector of a single grain (see inset in Fig. 1), by just through the angular average,

$$\langle M \rangle = \frac{1}{4\pi} \int_0^{2\pi} d\varphi \int_0^\pi M_L(\theta, \varphi) \sin \theta d\theta, \quad (2)$$

where θ and φ are the polar coordinates which characterize the orientation of the anisotropic grains with respect to H . In the case of the layered HTSC, one may assume just uniaxial anisotropy [the possible small differences between both in-plane (ab) magnetizations may be neglected, i.e., $M_a \approx M_b$]. In this case, if θ is chosen to be the angle between the c -crystallographic axis and the applied magnetic field (see inset in Fig. 1), Eq. (2) may be simplified to

$$\langle M \rangle = \int_0^{\pi/2} M_L(\theta) \sin \theta d\theta. \quad (3)$$

This angular average has been already used by Cho and co-workers¹⁵ to calculate the magnetization of randomly oriented polycrystals of highly anisotropic HTSC in the reversible mixed state. For that, these authors took into account that in these superconductors the out-of-plane magnetization (for H parallel to the ab layers) may be neglected in the mixed state, i.e., $M_c(T, H) \approx 0$. In this case, $M_L(\theta)$ is related

to the in-plane magnetization [for H perpendicular to the superconducting CuO_2 (ab) layers] of each crystalline grain by (see the inset in Fig. 1), $M_L(\theta) = M_{ab}(T, H \cos \theta) \cos \theta$. At the crossing point, i.e., for $T = T^*$, M_{ab} does not depend on H , and $M_L^*(\theta)$ is related to M_{ab}^* by just, $M_L^*(\theta) = M_{ab}^* \cos \theta$. By using this last expression and taking into account the background magnetization in real samples (see the Introduction),

$$\langle \Delta M^* \rangle = \frac{1}{2} \Delta M_{ab}^*, \quad (4)$$

a relationship first obtained by Cho and co-workers¹⁵ and that relates the excess magnetization at the crossing point in a randomly oriented polycrystalline HTSC sample to the corresponding crossing point excess magnetization of a single crystalline grain for H perpendicular to the ab planes.

The same procedure may be used to relate the field-cooled susceptibility in the Meissner state (for H below the lowest H_{c1}) of a polycrystalline HTSC, with randomly oriented single crystalline grains, $\langle \chi^{\text{FC}} \rangle$, to the field-cooled susceptibility of a single crystal with the ab planes oriented perpendicularly to H , χ_{ab}^{FC} . Let us stress already here, however, that there is an important conceptual difference in both cases: The relationships between $\langle M \rangle$ and M_{ab} in the mixed state, and in particular that of $\langle \Delta M^* \rangle$ and ΔM_{ab}^* through Eq. (4), are a direct consequence of the *intrinsic* anisotropy of the individual single crystalline grains ($\Delta M_{ab} \gg \Delta M_c$) and, therefore, they will apply in all the cases, even if these single crystalline grains were ideal, without any extrinsic inhomogeneity effect. However, in the case of an ideal single crystalline grain and neglecting also any demagnetizing or low dimensionality effect (this last being associated with the possible smallness of the grains relative to the superconducting characteristic lengths, see later), the susceptibility in the Meissner state will be always $\chi^{\text{FC}} = -1$, independently of the orientation of the grains relative to H . Therefore, a polycrystal with ideal single crystalline grains will also have $\langle \chi^{\text{FC}} \rangle = -1$. In other words, in such an ideal polycrystalline sample the Meissner effect is not affected by the random orientation of the grains, independently of their intrinsic anisotropy. In fact, one may directly reach such a conclusion by just taking into account that in the ideal Meissner state the applied magnetic field is fully expelled and the internal properties of the grains, as their anisotropy, are then irrelevant.

The almost trivial conclusions summarized above for $\langle \chi^{\text{FC}} \rangle$ in a polycrystalline superconductor, with randomly oriented anisotropic ideal single crystalline grains, will change dramatically if the Meissner expulsion of the magnetic field in each individual grain is affected by some extrinsic effects, as inhomogeneities or demagnetizing effects. In fact, these extrinsic effects, which will modify χ^{FC} of each grain from its ideal value of -1 , will be always present in some extent in real samples. In addition, it is reasonable to assume that in the case of strongly anisotropic superconductors, χ_{ab}^{FC} is different from χ_c^{FC} (for H parallel to the ab planes). Also, the demagnetizing effects, very relevant for values of H below the lower critical fields in HTSC (where the amplitudes of M and H are of the same order), will depend on the orientation of the grains relative to the applied magnetic field. In this case, the two components of the mag-

netization of each single crystalline grain, for H perpendicular and parallel to the ab planes, are given by, respectively,

$$M_{ab} = \frac{\chi_{ab}}{1 + \chi_{ab} D_{ab}} H_{ab} \quad (5)$$

and

$$M_c = \frac{\chi_c}{1 + \chi_c D_c} H_c, \quad (6)$$

where H_{ab} and H_c are the components of H in these two directions and D_{ab} and D_c are the corresponding demagnetizing factors of the individual grain. The projection of the magnetization vector along the H direction is then given by (see inset in Fig. 1),

$$\begin{aligned} M_L(\theta) &= M_{ab} \cos \theta + M_c \sin \theta \\ &= H \left(\frac{\chi_{ab}}{1 + \chi_{ab} D_{ab}} \cos^2 \theta + \frac{\chi_c}{1 + \chi_c D_c} \sin^2 \theta \right), \end{aligned} \quad (7)$$

which through Eq. (3) leads to

$$\langle \chi \rangle \equiv \frac{\langle M \rangle}{H} = \frac{1}{3} \left(\frac{\chi_{ab}}{1 + \chi_{ab} D_{ab}} + \frac{2\chi_c}{1 + \chi_c D_c} \right). \quad (8)$$

This equation relates the average (*measured*) susceptibility in a granular sample with randomly oriented single crystalline grains, with the susceptibilities and demagnetizing factors of the individual grains for H perpendicular and parallel to their ab layers. Note that if each grain would behave as an *ideal* superconductor, i.e., if the flux expulsion is total ($\chi_{ab}^{\text{FC}} = \chi_c^{\text{FC}} = -1$) and without demagnetizing effects ($D_{ab} = D_c = 0$), Eq. (8) will lead to $\langle \chi^{\text{FC}} \rangle = -1$, in agreement with the comments presented above.

In many real HTSC samples, Eq. (8) may be still simplified by taking into account that $|\chi_c^{\text{FC}}| \ll |\chi_{ab}^{\text{FC}}| < 1$. This is because, in these materials, the magnetic flux in this partial Meissner state is in general much more easily trapped for H parallel to the layers than in the perpendicular direction. Under these additional conditions Eq. (8) becomes

$$\langle \chi^{\text{FC}} \rangle \approx \frac{\chi_{ab}^{\text{FC}}}{3 + 3\chi_{ab}^{\text{FC}} D_{ab}}. \quad (9)$$

Moreover, usually each grain in a granular HTSC sample may be approximated as spherical (and then $D_{ab} = 1/3$) or ellipsoidal (and then, by assuming for instance an aspect ratio of $c/ab \approx 0.65$, well adapted to the grains of the samples measured in this work, $D_{ab} \approx 0.45$), which reduces Eq. (9) to

$$\langle \chi^{\text{FC}} \rangle \approx \frac{\chi_{ab}^{\text{FC}}}{3 + \chi_{ab}^{\text{FC}}}, \quad (10)$$

for spherical grains, or

$$\langle \chi^{\text{FC}} \rangle \approx \frac{\chi_{ab}^{\text{FC}}}{3 + 1.35\chi_{ab}^{\text{FC}}}, \quad (11)$$

for ellipsoidal grains with an aspect ratio of 0.65. For completeness, let us note that Eq. (9) will also apply to the so-called excess diamagnetism $\Delta \chi$ (associated with thermal

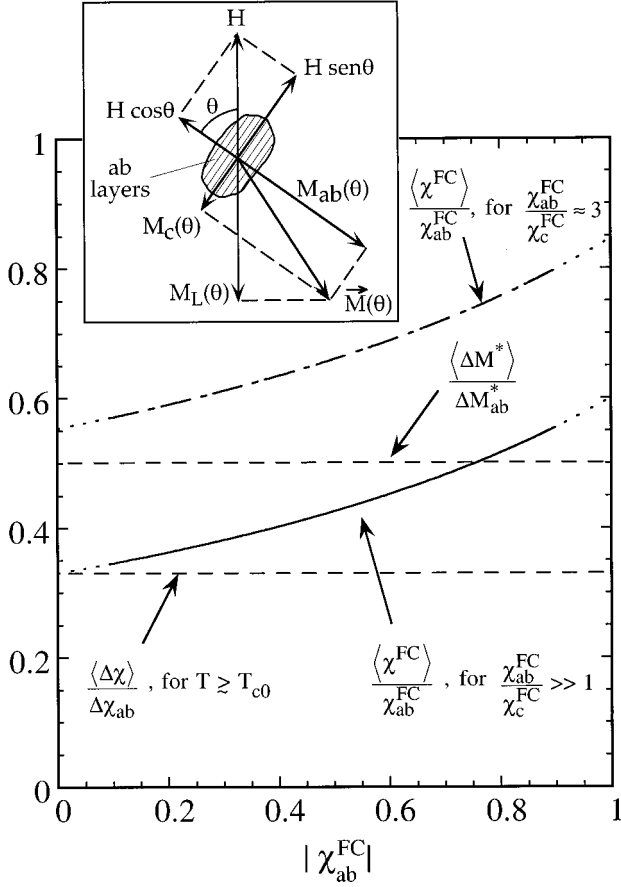


FIG. 1. Relative random orientation effects on the excess magnetization at the crossing point, $\langle \Delta M^* \rangle$, and on the field-cooled susceptibility in the Meissner state, $\langle \chi^{FC} \rangle$, versus χ_{ab}^{FC} , the field-cooled in-plane susceptibility of an individual grain. χ_{ab}^{FC} provides an estimation of the magnetic quality of the individual grains. The random orientation effects on $\langle \Delta M^* \rangle$ are due to the intrinsic anisotropy of the individual grains ($\Delta M_c \ll \Delta M_{ab}$) and, therefore, they are independent of the presence of extrinsic inhomogeneity effects (which reduce χ_{ab}^{FC}). In contrast, the extrinsic random orientation effects on $\langle \chi^{FC} \rangle$ will depend on the grains magnetic quality and, therefore, on χ_{ab}^{FC} . To obtain $\langle \chi^{FC} \rangle$, we have assumed ellipsoidal grains (with $D_{ab} = 0.45$ and $D_c = 0.27$) and different extrinsic anisotropies (due to an anisotropic flux trapping): The solid curve was obtained by assuming strong extrinsic anisotropy, i.e., $\chi_{ab}^{FC} / \chi_c^{FC} \gg 1$. The dot-dashed curve was obtained by assuming $\chi_{ab}^{FC} / \chi_c^{FC} \approx 3$, this last value corresponding to one of our samples. For completeness, it is indicated also the ratio of the excess diamagnetism, $\langle \Delta \chi \rangle / \langle \chi_{ab} \rangle$, associated with the creation, by thermal fluctuations, of Cooper pairs above but near T_c . In this case the random orientation effects are due to the intrinsic anisotropy of the layered HTSC (which leads to $\Delta \chi_{ab} / \Delta \chi_c \gg 1$).

fluctuations of Cooper pairs⁷) measured above T_c in granular anisotropic HTSC. In this region, $\langle M \rangle$ is also proportional to the applied magnetic field and $\Delta \chi_c \ll \Delta \chi_{ab}$, due in this case to the intrinsic anisotropy of the excess diamagnetism.⁷ In addition, in this region $|\Delta \chi_{ab}| \ll 1$, and Eq. (9) reduces to $\langle \Delta \chi \rangle = 1/3 \Delta \chi_{ab}$.

Figure 1 clearly illustrates some of the results obtained before for a granular sample with randomly oriented single crystalline grains. In this figure, we compare the behavior of the average excess magnetization at the crossing point (nor-

malized to ΔM_{ab}^*), $\langle \Delta M^* \rangle / \Delta M_{ab}^*$, and of the field-cooled susceptibility in the Meissner state (normalized to χ_{ab}^{FC}), $\langle \chi^{FC} \rangle / \chi_{ab}^{FC}$, as a function of the field-cooled in-plane susceptibility of each grain, χ_{ab}^{FC} , this last observable being to some extent a measure of the magnetic quality of each individual grain. The dotted parts of the $\langle \chi^{FC} \rangle / \chi_{ab}^{FC}$ curves just indicate that for very low and very high values of $|\chi_{ab}^{FC}|$ the extrinsic anisotropy condition, $|\chi_c^{FC}| < |\chi_{ab}^{FC}|$, will not be fulfilled and, therefore, Eqs. (9) to (11) will not be a good approximation. The random orientation effects on ΔM^* in granular samples are associated with the intrinsic anisotropy of the grains and, therefore, $\langle \Delta M^* \rangle / \Delta M_{ab}^*$ does not depend on the magnetic quality of each grain. In contrast, the random orientation effects on χ^{FC} are due to the extrinsic flux trapping anisotropy of each grain in the partial Meissner state, which is manifested only if the Meissner effect is incomplete, i.e., if both $|\chi_c^{FC}|$ and $|\chi_{ab}^{FC}|$ are less than one. In the $\langle \chi^{FC} \rangle / \chi_{ab}^{FC}$ curves in Fig. 1 we have assumed ellipsoidal grains, with an aspect ratio of the order of $c/ab = 0.65$ and two different extrinsic anisotropies: $\chi_{ab}^{FC} / \chi_c^{FC} = 3$ or $\chi_{ab}^{FC} / \chi_c^{FC} \gg 1$. As can be seen in this figure, in all cases these extrinsic random effects will affect more severely $\langle \chi^{FC} \rangle$ in the granular samples with low magnetic quality grains (with lower $|\chi_{ab}^{FC}|$).

The above results are of central importance for the comparison between the crossing point measurements in granular highly anisotropic HTSC and the theoretical approaches, because they allow an easy disentanglement of the different extrinsic effects on both $\langle \Delta M^* \rangle$ and $\langle \chi^{FC}(T^*) \rangle$. The crucial idea here is that, whereas the random orientation affects, as shown above, ΔM^* and $\chi^{FC}(T^*)$ in a very different way, the other extrinsic effects, associated with structural and stoichiometric inhomogeneities at different length scales affect both observables in a similar way, in spite of the fact that they are measured under very different magnetic field amplitudes [$H < H_{c1}(T^*)$ and, respectively, $H \leq H_{c2}(T^*)$; see next section]. In fact, this last hypothesis was fully confirmed by the direct measurements of both ΔM_{ab}^* and $\chi_{ab}^{FC}(T^*)$ in highly anisotropic HTSC single crystals performed in Ref. 14. Therefore, the intrinsic in-plane excess magnetization at the crossing point, corrected from inhomogeneity effects, is $-\Delta M_{ab}^* / \chi_{ab}^{FC}(T^*)$, which using the above results may be easily related to the measured observables in granular samples. For instance, from Eqs. (4) and (10) we found

$$-\frac{\Delta M_{ab}^*}{\chi_{ab}^{FC}(T^*)} = \frac{2\langle \Delta M^* \rangle}{3\langle \chi^{FC}(T^*) \rangle / (\langle \chi^{FC}(T^*) \rangle - 1)}, \quad (12)$$

which is a good approximation in the case of a sample with randomly oriented very anisotropic spherical (with $D_{ab} = D_c = 1/3$) single crystalline grains. Note that although the above estimations have been developed for independent single crystalline grains, they may also be a good approximation in the case of ceramic HTSC with weak Josephson coupled grains. This is because these weak couplings will be destroyed by the magnetic fields needed to perform the susceptibility measurements, even in the case of $\langle \chi^{FC} \rangle$, and each single crystalline grain may then behave as independent. Let us, finally, note also here that some attempts to correct through $\langle \chi^{FC} \rangle$ the crossing point measurements in

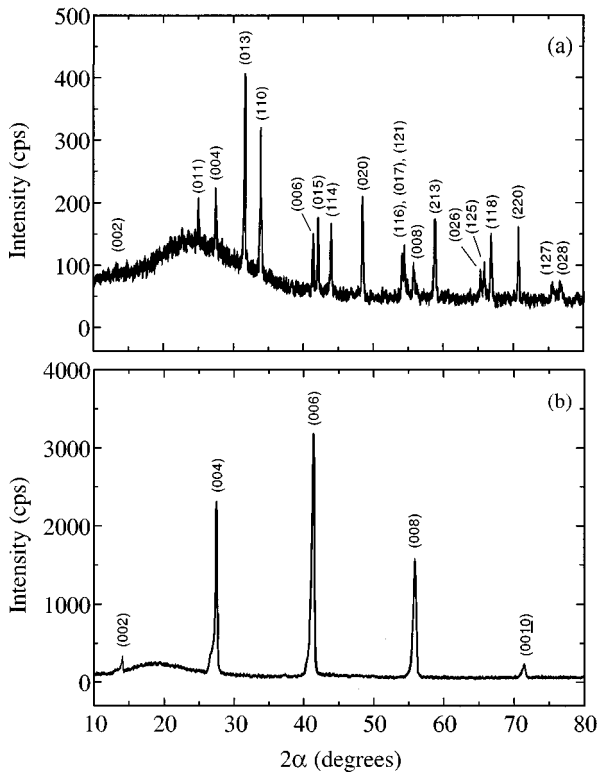


FIG. 2. X-ray diffraction patterns of the $L1$ powder sample before (a) and after (b) grain alignment. In the case of the randomly oriented sample, some of the peaks are hidden by the background and not indicated.

granular HTSC were already published by other groups.⁶ Unfortunately, due to an incorrect treatment of the random orientation effects, these authors erroneously concluded that such a procedure increases the disagreement between Eq. (1) and their measurements (see our comment in Ref. 6).

III. EXPERIMENTAL DETAILS AND RESULTS

The $\text{La}_{1.9}\text{Sr}_{0.1}\text{CuO}_4$ powder samples with randomly oriented grains were obtained by crushing pieces of the original crystals in an agate mortar. These crystals were synthesized by the *travelling solvent floating zone method* (TSFZ). Details of their synthesis and characterization may be found in Ref. 16. Let us only mention here that this method produces large twinned cylindrical crystals of typically 5 mm diameter and 80 mm long, with the a axis of the structure within a few degrees from the growth axis: two parallel ab -type flat faces running along the whole crystal are often observed. Particle size analysis (made with a Coulter Multisizer II analyzer) showed that the grains in the resulting powders have a mean diameter around 5–10 μm . The grain dimensions are, then, much bigger than the in-plane magnetic penetration depth and, indeed, than the superconducting coherence lengths, which are those that directly concern the thermal fluctuations of vortices. Therefore, we neglected any possible low-dimensionality effect on these vortex fluctuations associated with the grain dimensions. The x-ray diffraction patterns of these powders [see an example in Fig. 2(a)] show only the peaks corresponding to the $\text{La}_{1.9}\text{Sr}_{0.1}\text{CuO}_4$ phase. The magnetization measurements were made with a commercial

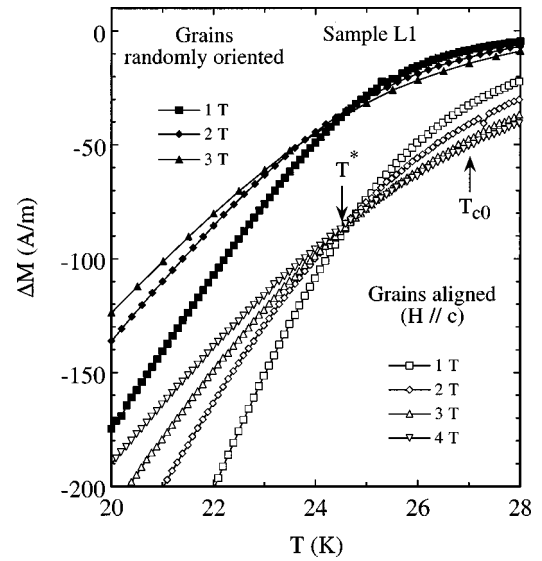


FIG. 3. Excess magnetization versus temperature curves around the transition for the powdered sample $L1$ before (closed data points) and after (open data points) grain alignment. In the second case the magnetic field was applied perpendicularly to the ab layers. The mean-field-like normal-superconducting transition temperature at zero applied magnetic field, T_{c0} , was estimated as the temperature where $\chi_c(T)$ (for H parallel to the ab layers) starts to decrease when the sample is cooled from the normal state (for details see the main text).

SQUID magnetometer (Quantum Design, model MPMS). The instrumental resolutions are 0.1% for the temperature, 10^{-11} A m^2 for the magnetic moment and $2 \times 10^{-6} \text{ g}$ for the sample mass. The resolution in the as-measured magnetization is then better than 5%. After the magnetization measurements were performed, the *same* powders were used to obtain grain aligned composites. To make the alignment, the powders were dispersed in low-magnetic susceptibility epoxy (EPOTEK 301) and held at a temperature of 300 K in a 5 T magnetic field during 15 h.¹⁷ The LaSCO volume fraction in the resulting epoxy matrix was near 20%. We have measured the magnetic moment of the epoxy alone: The resulting data show that its contribution to the magnetic moment in the grain oriented samples is less than 5%. The x-ray diffraction pattern of the grain-aligned sample [Fig. 2(b)] exhibits only the (001) peaks which indicates the excellent alignment of the grains. The measurements of the magnetization as a function of the sample orientation relative to the applied magnetic field were carried out with a commercial (Quantum Design) rotating sample holder that allows a relative precision of 0.1° in angle (see also the inset in Fig. 1).

A typical example of the excess magnetization versus temperature curves measured in one of the granular LaSCO samples before and after grain alignment is presented in Fig. 3. The solid points correspond to $\langle \Delta M(T)_H \rangle$ measured in the sample with the grains randomly oriented (noted $L1-R$), whereas the open data points are the $\Delta M_{ab}(T)_H$ data for the *same* sample after the grains have been aligned ($L1-A$). These measurements were performed with external magnetic field amplitudes within 1 T and 4 T. The crossing of the different $\langle \Delta M(T)_H \rangle$ and $\Delta M_{ab}(T)_H$ curves appears in both cases at a temperature $T^* \approx 24.5 \text{ K}$. In the case of the randomly oriented sample, the spread of T^* over a few tenths of

a degree is probably due, at least in part, to the fact that the different grains are under magnetic fields which cover different amplitudes perpendicular to the corresponding ab planes (see also Ref. 11). The excess magnetization amplitudes for the randomly oriented and grain aligned cases are, however, very different: $\langle \Delta M^* \rangle \approx -40$ A/m for $L1-R$, whereas $\Delta M_{ab}^* \approx -85$ A/m for $L1-A$. Let us notice already here that such a difference of nearly a factor two, provides an excellent confirmation of Eq. (4). The mean-field-like superconducting-normal transition temperature, T_{c0} , was estimated by measuring the magnetic susceptibility of the grain oriented samples with the magnetic field applied parallel to the ab layers of the grains. Under this field orientation, the thermal fluctuations of the Cooper pairs above the transition are negligible,¹⁸ and T_{c0} may be then approximated as the temperature where $\chi_c(T)$, measured with a relatively low magnetic field amplitude of 0.3 T, starts to decrease when the sample is cooled from the normal state.

The magnetic susceptibility versus temperature curves for the $L1$ sample before and after grain alignment are presented in Fig. 4. These susceptibility curves were obtained under field-cooled (FC) and zero-field-cooled (ZFC) conditions, in both cases by using an external magnetic field of 5×10^{-4} T, which is smaller than the lower critical fields (see later). These susceptibilities were calculated from the measured magnetization by just using the conventional definition, $\langle \chi \rangle = \langle M \rangle / H$. As it can be seen in Fig. 4(a), in the case of the sample with randomly oriented grains ($L1-R$), this procedure leads to absolute values of the shielding susceptibility, $\langle \chi^{ZFC} \rangle$, bigger than one at low temperatures. This unphysical result is due to the fact that the above definition applies only in the ideal case and does not take into account either the demagnetizing effects or the random orientation effects. These last random orientation effects are present even in this zero-field-cooled case because the partial magnetic field penetration is also anisotropic, due to the strong anisotropy of the magnetic field penetration length of these materials. Therefore, it is not possible to overcome these extrinsic effects by just using a conventional expression for the magnetic susceptibility in single crystals that takes only the demagnetization effects into account [as, for instance, through $\langle \chi \rangle = \langle M \rangle / (H - D \langle M \rangle)$, as proposed in Ref. 6]. An analysis of these extrinsic effects on the zero-field-cooled susceptibility of Fig. 4(a) in terms of the approaches summarized in Sec. II is going to be presented in the next section. Moreover, in Fig. 4(a) we see that the field-cooled susceptibility, $\langle \chi^{FC} \rangle$, is only 20% of the corresponding $\langle \chi^{ZFC} \rangle$. As already discussed in Sec. II, these differences are mainly due to the magnetic flux trapped by the different stoichiometric and structural inhomogeneities.

The magnetic susceptibility versus temperature for the same sample but after its grains have been aligned (sample $L1-A$) is presented in Figs. 4(b) and 4(c) for the magnetic field applied perpendicular and, respectively, parallel to the ab layers. These measurements were also performed under FC and ZFC conditions with a magnetic field amplitude of again 5×10^{-4} T. In this case, there are no random orientation effects and the susceptibilities may be then calculated from the measured magnetization through the conventional expressions, Eqs. (5) and (6), which take into account the corresponding demagnetization factor. In what concerns Fig.

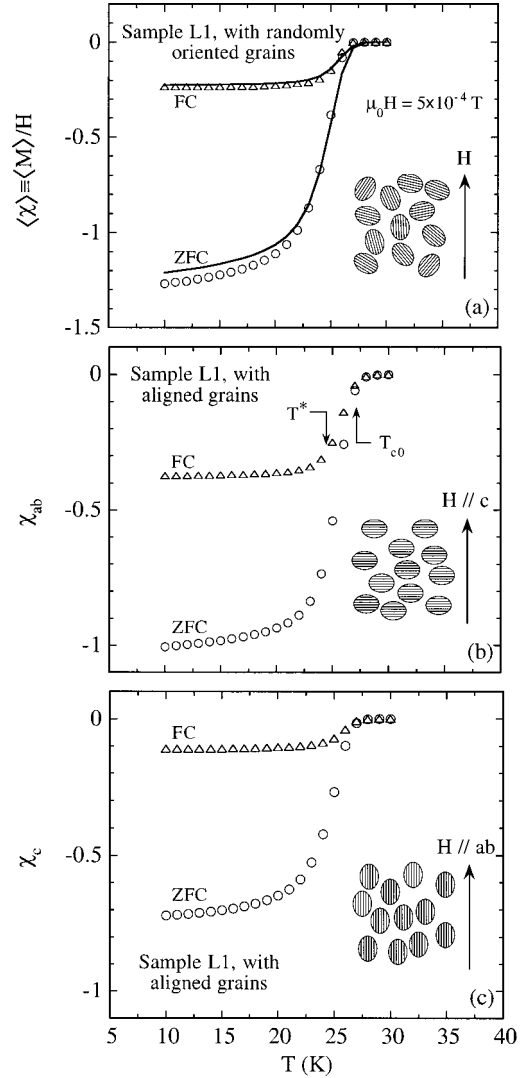


FIG. 4. Magnetic susceptibility versus temperature curves for sample $L1$, measured under FC and ZFC conditions with a magnetic field of 5×10^{-4} T, which is smaller than the lower critical magnetic fields. The data in (a) were taken before grain alignment (i.e., with the grains randomly oriented). The data in (b) and (c) were taken after grain alignment, with the magnetic applied perpendicular and, respectively, parallel to the ab layers. These last data have been corrected for demagnetizing effects through Eqs. (5) and (6) and by imposing $\chi^{ZFC}(T \rightarrow 0) = -1$, as explained in the main text.

4(b), the central point to be stressed is that in the saturated low temperature region we have imposed $\chi_{ab}^{ZFC}(T \rightarrow 0)$ to be equal to -1 . This is because the magnetic penetration length for the in-plane shielding currents, λ_{ab} , is in these compounds around 500 nm,¹⁹ a value much smaller than the mean grains size (5–10 μm). So, by imposing $\chi_{ab}^{ZFC}(T \rightarrow 0) = -1$ in Eq. (5) we found for sample $L1$, $D_{ab} \approx 0.45$, which corresponds to an aspect ratio for the grains of $c/ab \approx 0.65$.²⁰ Such a value is reasonable in view of the structural anisotropy of the material. Moreover, through the relation $D_{ab} + 2D_c = 1$, this D_{ab} value leads to $D_c \approx 0.275$.²⁰ As we can see in Fig. 4(b), χ_{ab}^{FC} is only 35% of χ_{ab}^{ZFC} . As stressed before, these lower values of χ_{ab}^{FC} are due to magnetic flux trapping by inhomogeneities.

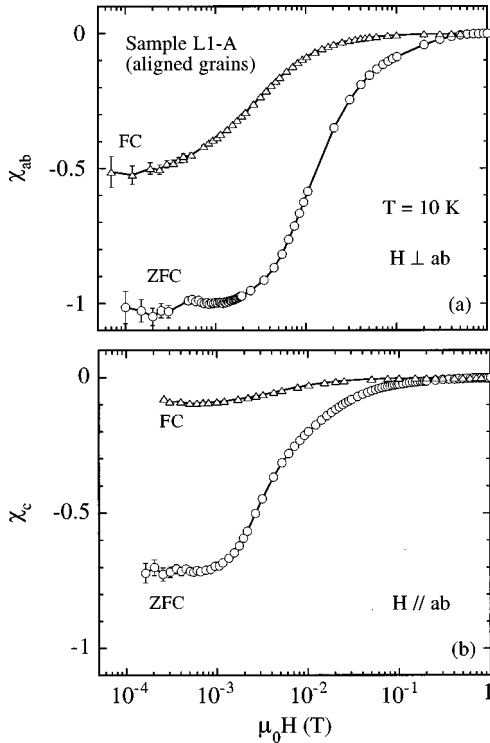


FIG. 5. Magnetic susceptibility versus external magnetic field for sample *L1* after the grains have been aligned, measured under FC and ZFC conditions at a temperature of 10 K. The data in (a) and (b) were obtained with the magnetic field applied perpendicularly and, respectively, parallel to the *ab* layers. The solid lines are guides for the eye.

As can be seen in Fig. 4(c), for H parallel to the *ab* planes, χ_c^{ZFC} saturates at low temperature at a value around -0.7 , which is well below that corresponding to χ_{ab}^{ZFC} . This may be easily understood by considering that the magnetic penetration length for the shielding currents flowing perpendicularly to the *ab* planes, λ_c , is around $2 \mu\text{m}$ at low temperatures,¹⁹ a value that is of the order of that of the grains size. It can also be seen in this figure, finally, that χ_c^{FC} has absolute values much smaller than χ_{ab}^{FC} . In this case, this may be due to the layered structure of the material, which again makes the magnetic flux to be much strongly trapped during the field-cooling process for $H \parallel ab$ than for $H \perp ab$.

All through the above analyses in the Meissner state we have assumed that the magnetic susceptibilities are independent of H . When the Meissner expulsion is only partial, this could not be always the case due to nonlinear flux trapping effects.²¹ So, it is crucial for the validity of our analysis to check that the measurements were performed not only for magnetic fields below H_{c1} , the lower critical magnetic field, but also in the linear region, i.e., in the region where χ is independent of H . For that, we have performed detailed measurements of the magnetic susceptibility under field-cooled and zero-field-cooled conditions, versus the external magnetic field. Two examples corresponding to the sample *L1* after the grains have been aligned and for a temperature of 10 K, are presented in Fig. 5(a) for $H \perp ab$ and in Fig. 5(b) for $H \parallel ab$. Let us remark that these FC measurements have been performed by fulfilling the FC conditions for *each* data

point, i.e., each data point was obtained by heating the sample above the transition, and then cooling it again in presence of the new magnetic field amplitude. As can be seen in these figures, both χ_{ab}^{ZFC} and χ_c^{ZFC} are almost H -independent up to $\mu_0 H = 2 \times 10^{-3}$ T and 10^{-3} T, respectively (values which may be related to the corresponding lower critical magnetic field amplitudes). As commented above, the field-cooled susceptibilities, χ_{ab}^{FC} and χ_c^{FC} , are slightly H -dependent below these last magnetic field values. However, they tend to a saturation value as H decreases, and for $\mu_0 H = 5 \times 10^{-4}$ T (the magnetic field amplitude used in the measurements presented in Fig. 4) they are already almost H independent. Note that the small discrepancies between the data of Figs. 3 and 4 [of the order of 10% in the case of $\chi_{ab}^{\text{FC}}(T = 10 \text{ K})$] are due to the uncertainties when correcting the remanent field of the magnetometer superconducting coil.

IV. DISCUSSION

Let us first comment on our experimental results on the crossing point of the excess magnetization versus temperature curves of Fig. 3. As we have already noted in the previous section, it can be easily seen in that figure that the magnetization at the crossing point for the sample with the grains randomly oriented (*L1-R*) takes an absolute value which is nearly one half that corresponding to the same sample after the grains have been aligned (*L1-A*). This result, which is also obtained for the other sample (see Table I), provides a quantitative confirmation of the random orientation effects on the crossing point in highly anisotropic HTSC [Eq. (4)]. However, even in the case of the grain-aligned sample (without, then, random orientation effects), the crossing point coordinates do not agree with the theoretical predictions [Eq. (1)]. In fact, using in Eq. (1) $T^* = 24.5 \text{ K}$ (which, due to the spread of the crossing point, is determined with an accuracy around 0.3 K) and a periodicity length for the vortex fluctuations of $s_e^V = s = 6.6 \text{ \AA}$, we obtain $\Delta M_{ab}^* = -248 \text{ A/m}$, a value three times larger than the measured one. A similar discrepancy has been observed for the other grain-aligned sample studied here (see Table I). The central point here is that, as can be seen from Fig. 4(b), such a disagreement is almost the same as the shift between $\chi_{ab}^{\text{FC}}(T^*)$ and its ideal value of -1 : For this sample, $|\Delta M_{ab}^* / \chi_{ab}^{\text{FC}}(T^*)| = -280 \text{ A/m}$, i.e., exhibiting a difference with the theoretical prediction well within the experimental uncertainties (of the order of 10%). Such a result, that has also been observed in the other grain aligned sample (see Table I), confirms that $|\Delta M_{ab}^* / \chi_{ab}^{\text{FC}}(T^*)|$ is the intrinsic magnetization of the crossing point, as first noted in Ref. 14 in the case of single crystal samples. In other words, once the random orientation effects have been corrected, the extrinsic effects on $\chi_{ab}^{\text{FC}}(T^*)$ and on ΔM_{ab}^* are almost similar, in spite of the fact that these observables are measured under very different magnetic field amplitudes [$H < H_{c1}(T^*)$ and $H \lesssim H_{c2}(T^*)$]. These results suggest the presence in the individual single crystalline grains of structural and stoichiometric inhomogeneities, too small to be observed by conventional techniques (as, e.g., conventional x-ray diffraction), but that may appreciably affect in a similar way both observables.

TABLE I. Values of some of the parameters related to the thermal fluctuation effects of the two polycrystalline LaSCO samples studied here. The mean-field transition temperature was determined by the onset of the diamagnetic transition for H parallel to the ab planes in the grain-aligned samples. The other parameters are defined in the main text. The errors in the in-plane excess magnetization values are estimated to be no more than 10% whereas for the in-plane susceptibility, due to the demagnetization factors, the errors are estimated to be no more than 15%.

Sample	T_{c0} (K)	T^* (K)	$\langle \Delta M^* \rangle$ or ΔM_{ab}^* (A/m)	$\langle \chi^{\text{FC}}(T^*) \rangle$ or $\chi_{ab}^{\text{FC}}(T^*)$	Theoretical ΔM_{ab}^* (A/m)	$\Delta M_{ab}^* / \chi_{ab}^{\text{FC}}(T^*) $ (A/m)
L1	27.1	24.5	randomly oriented	-0.20	-248	-280
			grain-aligned	-0.30	-85	
L2	28.0	25.0	randomly oriented	-0.15	-253	-220
			grain-aligned	-0.30	-65	

As a complementary but important check of the adequacy of the above analyses, the solid lines in Fig. 4(a) have been obtained by using the data of Figs. 4(b) and 4(c) in Eq. (8). As can be seen in that figure, the agreement with the measured $\langle \chi \rangle$, under both field-cooled and zero-field-cooled conditions, is excellent, the small deviation, in both cases of less than 10%, being mainly due to the uncertainties in the determination of the demagnetizing coefficients. These results show, therefore, that in spite of the entanglement of the intrinsic and extrinsic effects on $\langle \chi^{\text{FC}} \rangle$ and $\langle \chi^{\text{ZFC}} \rangle$, both observables still obey the usual vectorial composition of the magnetization which leads to Eq. (8). Let us stress here again that the extrinsic random orientation effects on χ^{FC} are due to the flux trapping anisotropy of the grains, whereas in the case of χ^{ZFC} these random effects are mainly due to the anisotropy of the penetration depth.

As a further illustration of the random orientation effects on the magnetization in granular HTSC, in Fig. 6 we present an example corresponding to sample L1-A, of the longitudinal magnetization, M_L , versus the angle between the c direction and the applied magnetic field (see inset in Fig. 1), for $\mu_0 H = 5 \times 10^{-4}$ T and $T = 10$ K under FC and ZFC conditions. Note that the FC measurements have been performed by fulfilling the FC conditions for *each* angle, i.e., each data point was obtained by heating the sample above the transition, rotating it to the following angle, and then cooling it again in presence of the magnetic field.²² As expected, $M_L(\theta)_{T,H}$ follows the θ dependence of Eq. (7) (solid lines) at a quantitative level for both the ZFC and the FC cases. These lines were calculated by using for χ_{ab}^{ZFC} , χ_{ab}^{FC} , χ_c^{ZFC} , and χ_c^{FC} the experimental values (for $T = 10$ K and $\mu_0 H = 5 \times 10^{-4}$ T) already shown in Figs. 4 or 5, and by using also $D_{ab} = 0.45$ and $D_c = 0.275$ for the demagnetization factors, as explained in the previous section. Let us remember here that in the ZFC measurement the angle dependence of M_L is due to the *intrinsic* anisotropy of the penetration length, that is, the magnetic field penetrates deeper in the grains when H is applied parallel to the ab layers ($\theta = 90^\circ$). Instead, in the FC measurement, these differences are due to the *extrinsic* anisotropy in the flux trapping during the field-cooling process. In addition, the differences in M_L for $\theta = 0^\circ$ and $\theta = 90^\circ$ are amplified by the demagnetizing

effect, which is smaller for this last field orientation due to the usual ellipsoidal shape of the grains.

Finally, let us note here that we have also checked that the $\Delta M_{ab}(T, H) / |\chi_{ab}^{\text{FC}}(T^*)|$ data obtained in aligned grain samples obey, at least at a qualitative level, the explicit scaling function proposed by Tešanović and co-workers.⁹ In doing this comparison, the in-plane superconducting-coherence-length amplitude was crudely estimated by comparing the magnetization data above T_{c0} with the theoretical excess diamagnetism associated with the Cooper pairs created by thermal fluctuations.¹⁸ These last results extend to grain-oriented highly-anisotropic HTSC our previous quantitative findings obtained in TI-2223 crystals (see third paper in Ref. 7). In this last case the agreement with the scaling

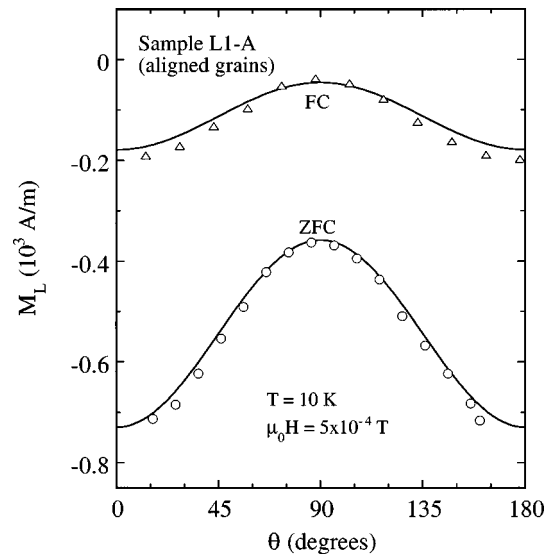


FIG. 6. Field-cooled and zero-field-cooled longitudinal magnetization, M_L , versus the angle between the applied magnetic field and the c -crystallographic axis (see inset in Fig. 1) for the grain-aligned sample L1-A. These measurements were performed at a temperature of 10 K and with an external magnetic field of 5×10^{-4} T which, for this sample, is well below the lower critical magnetic fields (see Fig. 5). As can be seen, the data follow at a quantitative level the angular dependence predicted by Eq. (7) (solid lines).

function of Tešanović and co-workers was excellent. New magnetization measurements above and below T_{c0} in different HTSC granular samples will be necessary to confirm at a quantitative level these results and also to determine the scaling behavior in randomly oriented granular samples. Note, however, that in LaSCO samples this type of scaling may be affected by the loss of the 2D behavior for temperatures close to T_c .

V. CONCLUSIONS

In conclusion, the experimental results and the analyses presented in this paper provide unambiguous answers to the questions addressed in the Introduction: In a granular HTSC, with randomly oriented anisotropic single crystalline grains, both the measured magnetization at the crossing point and the Meissner fraction are strongly affected by random orientation effects. In the case of the magnetization at the crossing point these effects are intrinsic and due to the anisotropy of the individual single crystalline grains. In contrast, for the Meissner fraction the random orientation effects are extrinsic and due to the fact that in real single crystalline HTSC the partial flux expulsion depends on the relative orientation between the ab planes and the applied magnetic field. These last effects have been estimated as a function of the measured susceptibilities in each direction and also of the corresponding demagnetization factors. Then, it was shown that once these random orientation effects are taken into account separately and independently for $\langle \Delta M^* \rangle$ and $\langle \chi^{\text{FC}}(T^*) \rangle$ [and also the demagnetization effects in the case of $\langle \chi^{\text{FC}}(T^*) \rangle$], both observables are affected in a similar way by the other extrinsic effects associated with different inhomogeneities at different length scales. Our results here and in Ref. 14 strongly suggest that these last extrinsic effects are mainly due to the presence of important nonsuperconducting domains in the apparently very good samples, in spite of the fact that in some cases they are not observed by x-ray diffraction. These stoichiometric inhomogeneities will, therefore, affect in the same way $\langle \Delta M \rangle$ and $\langle \chi \rangle$. In other words,

as is the case in single crystalline samples,¹⁴ the resulting $\Delta M_{ab}^*/|\chi_{ab}^{\text{FC}}(T^*)|$ is also the intrinsic excess magnetization at the crossing point in granular HTSC. Then, it was shown that it is this intrinsic excess magnetization at the crossing point that obeys Eq. (1), with $s_e^V = s$. Let us stress here again, however, that we have observed that the corrections of the inhomogeneity effects on $\Delta M_{ab}^*(T^*)$ through $\chi_{ab}^{\text{FC}}(T^*)$ do not always apply in the case of samples with a very deficient magnetic quality, let us say with $\chi_{ab}^{\text{FC}}(T^*)$ below about 0.2. For these low-quality samples one may expect that the flux trapping will depend on the magnetic field amplitude. So, in these cases the structural inhomogeneities may affect quite differently ΔM_{ab}^* and $\chi_{ab}^{\text{FC}}(T^*)$.

The results presented here extend to polycrystalline and granular HTSC with randomly oriented single crystalline grains and domains, our previous conclusions on the crossing point of the magnetization versus temperature curves obtained in single crystals: Once the different extrinsic effects are disentangled, the crossing point effect observed in highly anisotropic HTSC may be explained, even in granular samples, in terms of thermal fluctuations of vortices, as proposed by the BLK and the TXBLS approaches.^{8,9,11} The adequacy of our treatments of the random orientation effects is also confirmed at a quantitative level by comparing our measurements of $\langle \Delta M^* \rangle$ and $\langle \chi^{\text{FC}}(T^*) \rangle$ in granular samples after and before grain alignment. In addition to their interest for the understanding of the vortex fluctuation effects in highly anisotropic HTSC, these results may also be useful for a better understanding of other aspects of the magnetization in polycrystalline and granular HTSC.

ACKNOWLEDGMENTS

This work was based in part on the Ph.D. thesis of Jesús Mosqueira (University of Santiago de Compostela, Spain, 1997) and was supported by the Comisión Interministerial de Ciencia y Tecnología of Spain under Grant Nos. MAT95-0279 and MAT98-0371.

¹K. Kadowaki, *Physica C* **185–189**, 2249 (1991).

²P. H. Kes, C. J. van der Beck, M. P. Maley, M. E. McHenry, D. A. Huse, M. J. V. Menken, and A. A. Menovsky, *Phys. Rev. Lett.* **67**, 2383 (1991).

³Q. Li, M. Suenaga, T. Hikata, and K. Sato, *Phys. Rev. B* **46**, 5857 (1992); Q. Li, K. Shibusaki, M. Suenaga, I. Shigaki, and R. Ogawa, *ibid.* **48**, 9877 (1993); Q. Li, M. Suenaga, L. N. Bulaeviskii, T. Hikata, and K. Sato, *ibid.* **48**, 13 865 (1993); Q. Li, M. Suenaga, G. D. Gu, and N. Koshizuka, *ibid.* **50**, 6489 (1994); J. R. Thompson, J. G. Ossandon, D. K. Christen, B. C. Chakoumakos, Yang Ren Sun, M. Paranthaman, and J. Brynstad, *ibid.* **48**, 14 031 (1993); Z. J. Huang, Y. Y. Xue, R. L. Meng, X. D. Qiu, Z. D. Hao, and C. W. Chu, *Physica C* **228**, 211 (1994); N. Kobayashi, K. Egawa, K. Miyoshi, H. Iwasaki, H. Ikeda, and R. Yoshizaki, *ibid.* **219**, 265 (1994); R. Jin, H. R. Ott, and A. Schilling, *ibid.* **228**, 401 (1994); G. Triscone, A. F. Khoder, C. Opagiste, J.-Y. Genoud, T. Graf, E. Janod, T. Tsukamoto, M. Couch, A. Junod, and J. Muller, *ibid.* **224**, 263 (1994); A.

Wahl, A. Maignan, C. Martin, V. Hardy, J. Provost, and Ch. Simon, *Phys. Rev. B* **51**, 9123 (1995); Y. Y. Xue, Y. Cao, Q. Xiong, F. Chen, and C. W. Chu, *ibid.* **53**, 2815 (1996); G. Villard, D. Pelloquin, A. Maignan, and A. Wahl, *Physica C* **278**, 11 (1997).

⁴Q. Li, M. Suenaga, T. Kimura, and K. Kishio, *Phys. Rev. B* **47**, 11 384 (1993).

⁵B. Janossy, L. Fruchter, I. A. Campbell, J. Sanchez, I. Tanaka, and H. Kojima, *Solid State Commun.* **89**, 433 (1994). The values of ΔM^* and T^* found by these authors lead, when compared with Eq. (1), to an effective layering periodicity of 42 Å, which is more than 6 times the crystallographic periodicity of the superconducting CuO₂ layers. Such a discrepancy was attributed by these authors to an intrinsic weak two-dimensional character of the LaSCO samples, although it may be easily understood in terms of extrinsic inhomogeneities which decrease the measured ΔM^* .

⁶J.-Y. Genoud, G. Triscone, A. Junod, T. Tsukamoto, and J.

- Muller, *Physica C* **242**, 143 (1995). It was concluded in this paper that any correction for extrinsic inhomogeneity effects through the measured Meissner fraction will increase the disagreement between the excess magnetization at the crossing point that they measure in ceramic $\text{Bi}_2\text{Sr}_2\text{CaCu}_2\text{O}_8$ (Bi-2212) samples and the theoretical prediction [Eq. (1)]. It seems that these authors arrive at this conclusion because they do not correct the measured field-cooled magnetization from random orientation effects. Instead, they introduce only a correction for demagnetizing effects, and in addition through an expression which is applicable only to single crystals or grain aligned samples. Such a correction, is equivalent to use in Eq. (12), $\langle\chi^{\text{FC}}(T^*)\rangle/(0.16\langle\chi^{\text{FC}}(T^*)\rangle-1)$ instead of $3\langle\chi^{\text{FC}}(T^*)\rangle/(\langle\chi^{\text{FC}}(T^*)\rangle-1)$. This leads to very different values of the correction factor in Eq. (12). Although Eq. (12) applies only to randomly oriented *uncoupled* grains, it may also be a reasonable approximation for ceramic samples provided that the applied magnetic field has enough amplitude to decouple the grains. This seems to be the case in the measurements of these authors. For instance, for the ceramic Bi-2212 sample noted ‘‘ceram-2,’’ whose data are given in Figs. 2 and 5 of the Genoud *et al.* paper, $\langle\chi^{\text{FC}}(T^*)\rangle \approx -1/2$, which through Eq. (12) leads to a correction factor of the order of 1, whereas the procedure proposed by these authors leads to a correction factor of the order of 0.4. Such a difference, somewhat larger than a factor of 2, is just the disagreement factor claimed by these authors between their data and the theoretical proposal [Eq. (1)].
- ⁷J. Mosqueira, E. G. Miramontes, C. Torrón, J. A. Campá, I. Rasines, and F. Vidal, *Phys. Rev. B* **53**, 15 272 (1996); J. Mosqueira, M. V. Ramallo, A. Pomar, C. Torrón, and F. Vidal, *J. Low Temp. Phys.* **105**, 1111 (1996); J. Mosqueira, A. Maignan, Ch. Simon, C. Torrón, A. Wahl, and F. Vidal, *Physica C* **282–287**, 1539 (1997).
- ⁸L. N. Bulaevskii, M. Ledvig, and V. G. Kogan, *Phys. Rev. Lett.* **68**, 3773 (1992).
- ⁹Z. Tešanović, L. Xing, L. N. Bulaevskii, Q. Li, and M. Suenaga, *Phys. Rev. Lett.* **69**, 3563 (1992). See also Z. Tešanović and A. V. Andreev, *Phys. Rev. B* **49**, 4064 (1994).
- ¹⁰See, e.g., M. Tinkham, *Introduction to Superconductivity* (McGraw-Hill, New York, 1996), Chaps. 8 and 9.
- ¹¹In the case of the BLK approach (Ref. 8), applicable in the low magnetic field limit [$H \ll H_{c2}(T^*)$], there is a prefactor on the right side of Eq. (1) which depends on the structure of the vortex lattice and on the vortex core. However, this prefactor is predicted to be of the order of one, and the corresponding correction is in general well within the experimental accuracy, mainly in the case of polycrystalline samples where due to their random orientations the different grains are under magnetic fields which cover different amplitudes perpendicular to the corresponding ab planes.
- ¹²A. E. Koshelev, *Phys. Rev. B* **50**, 506 (1994).
- ¹³A. Junod, J. Y. Genoud, G. Triscone, and T. Schneider, *Physica C* **294**, 115 (1998). In this paper it is proposed that the crossing point of the $\Delta M(T)_H$ curves, for different values of H , is located just at the normal-superconducting transition, i.e., that $T^* = T_{c0}$. However, our susceptibility measurements for $H < H_{c1}$ clearly show [see, e.g., Fig. 4(b)] that for $T = T^*$ the corresponding in-plane field-cooled susceptibility, $\chi_{ab}^{\text{FC}}(T^*)$, is already in the saturated part of the $\chi_{ab}(T)$ curves, i.e., $\chi_{ab}^{\text{FC}}(T^*) = \chi_{ab}^{\text{FC}}(T \rightarrow 0)$. These $\chi_{ab}^{\text{FC}}(T)$ curves also clearly show that T^* is always well below (by a few degrees) the drop of the susceptibility at the diamagnetic transition. In fact, our previous measurements in different high-quality HTSC crystals (see Refs. 7 and 14) clearly show that, at least for the $\Delta M(T)_H$ curves obtained in relatively high magnetic fields (i.e., $\mu_0 H \geq 1$ T), T^* is always below T_{c0} , estimated as the temperature where $\chi_c(T)$, which is not appreciably affected by thermal fluctuations, drops when approaching the transition from above. Only in samples exhibiting broad transitions (due to stoichiometric inhomogeneities), the $\Delta M(T)_H$ curves for some values of H below $H_{c1}(T^*)$ may pass, *just by chance*, through the crossing point (as it is the case for the results presented in that paper) and then some ambiguities about the location of T^* relative to T_{c0} may arise. Indeed, even in the case of low quality samples, for other values of H (always below H_{c1}) the $\Delta M(T)_H$ curves, which in this partial Meissner state must be proportional to H , will not cross at all at the same point.
- ¹⁴J. Mosqueira, J. A. Campá, A. Maignan, I. Rasines, A. Revcolevschi, C. Torrón, J. A. Veira, and F. Vidal, *Europhys. Lett.* **42**, 461 (1998).
- ¹⁵J. H. Cho, D. C. Johnston, M. Ledvig, and V. G. Kogan, *Physica C* **212**, 419 (1993).
- ¹⁶A. Revcolevschi and J. Jegoudez, in *Coherence in High T_c Superconductors*, edited by G. Deutscher and A. Revcolevschi (World Scientific, Singapore, 1996), p. 19.
- ¹⁷D. E. Farrell, B. S. Chandrasekhar, M. M. Fang, V. G. Kogan, J. R. Clem, and D. K. Finnemore, *Phys. Rev. B* **36**, 4025 (1987).
- ¹⁸M. V. Ramallo, C. Torrón, and F. Vidal, *Physica C* **230**, 97 (1994).
- ¹⁹T. Shibauchi, H. Kitano, K. Uchinokura, A. Maeda, T. Kimura, and K. Kishio, *Phys. Rev. Lett.* **72**, 2263 (1994).
- ²⁰J. A. Osborn, *Phys. Rev.* **67**, 351 (1945).
- ²¹L. Krusin-Elbaum, A. P. Malozemoff, D. C. Cronmeyer, F. Holtzberg, J. R. Clem, and Z. Hao, *J. Appl. Phys.* **67**, 4670 (1990).
- ²²If the measurement is performed by first field cooling the sample and then taking the data as the sample is rotated [see, e.g., S. K. Hasanain, S. Manzoor, and M. Aftab, *Physica C* **272**, 43 (1996)], the flux trapped during the field-cooling process would rotate solidarily with the sample, resulting in an erroneous measurement of the true FC magnetization.